Molecular activated recombination in divertor simulation plasma on GAMMA 10/PDX

著者	Sakamoto M., Terakado A., Nojiri K., Ezumi N., Nakashima Y., Sawada K., Ichimura K., Fukumoto M., Oki K., Shimizu K., Ohno N., Masuzaki S., Togo S., Kohagura J., Yoshikawa M.
journal or publication title	Nuclear materials and energy
volume	12
page range	1004-1009
year	2017-08
権利	(C)2017 The Authors. Published by Elsevier Ltd. This is an open access article under the CC BY-NC-ND license. (http://creativecommons.org/licenses/by-nc-nd/4.0/)
URL	http://hdl.handle.net/2241/00149881

doi: 10.1016/j.nme.2017.05.001

Nuclear Materials and Energy 12 (2017) 1004–1009

Contents lists available at ScienceDirect

Nuclear Materials and Energy

journal homepage: www.elsevier.com/locate/nme

Molecular activated recombination in divertor simulation plasma on GAMMA 10/PDX

M. Sakamoto[a,*], A. Terakado[a], K. Nojiri[a], N. Ezumi[a], Y. Nakashima[a], K. Sawada[b], K. Ichimura[a], M. Fukumoto[c], K. Oki[d], K. Shimizu[a], N. Ohno[e], S. Masuzaki[f], S. Togo[a], J. Kohagura[a], M. Yoshikawa[a]

[a] Plasma Research Center, University of Tsukuba, 1-1-1 Tennodai, Tsukuba, Ibaraki 305-8577, Japan
[b] Faculty of Engineering, Shinshu University, 4-17-1 Wakasato, Nagano 380-8553, Japan
[c] National Institutes for Quantum and Radiological Science and Technology, 801-1, Mukoyama, Naka, Ibaraki 311-0193, Japan
[d] Graduate School of Electrical and Electronic Engineering, Chiba University, Chiba 263-8522, Japan
[e] Graduate School of Engineering, Nagoya University, Furo-cho, Chikusa-ku, Nagoya 464-8603, Japan
[f] National Institute for Fusion Science, 322-6 Oroshi-cho, Toki 509-5292, Japan

ARTICLE INFO

Article history:
Received 26 July 2016
Revised 26 April 2017
Accepted 2 May 2017
Available online 16 May 2017

ABSTRACT

In the tandem mirror GAMMA 10/PDX, molecular activated recombination (MAR) leading to plasma detachment has been observed by additional hydrogen gas injection to the divertor simulation plasma (i.e. end loss plasma) which is exposed to the V-shaped target in the divertor simulation experimental module (D-module). The temperature near the corner of the V-shaped target decreased from ~23 eV to ~2 eV as the neutral pressure in the D-module increased. A clear density rollover was observed at ~2 Pa. A position of the density maximum moves to upstream of the plasma with increase in the neutral pressure and the density near the corner of the target decreases to detach the plasma from the target. After the occurrence of the density rollover, the Balmer β intensity decreases as with the density but the Balmer α intensity continues to increase, indicating the dissociative attachment process in MAR is more dominant than the ion conversion process although the rate coefficient of the former process is lower than that of the latter one, which is calculated by using a collisional radiative model. This would be caused by the MAR process related to triatomic hydrogen molecules which significantly contributed to the detachment process.

1. Introduction

One of the important problems for magnetic fusion devices is to significantly reduce heat load on a divertor plate to prevent plasma-facing components from damage. Plasma detachment at the divertor plate is considered to be the most promising solution to this problem. A significant power out of the core plasma comes to the divertor region through a scrape-off layer and it is reduced by dissipative radiation and inelastic collisions due to plasma–gas interaction including atomic and molecular processes to decrease in plasma temperature. When the electron temperature decreases below a certain value, volumetric recombination can play an important role in the reduction of particle flux towards the divertor plate and the plasma is detached form the divertor plate. The volumetric recombination can occur through molecular activated recombination (MAR) as well as electron ion recombination (EIR). The MAR processes for the plasma detachment have been studied theoretically [1-7], and experimentally in linear machines [8-13] and tokamaks [14-15].

In the tandem mirror GAMMA 10/PDX, recently, a new project has been promoted to study the boundary plasma and plasma surface interaction (PSI) [16-18]. The divertor simulation experimental module (D-module) has been installed in the end region of the mirror device to make best use of a linear plasma device with plasma confinement. Molecular activated recombination leading to plasma detachment has been observed by additional hydrogen gas injection to the divertor simulation plasma. In the present paper, the MAR processes in the divertor simulation plasma are investigated comparing experimental results and a collisional radiative (CR) model. It is suggested that triatomic hydrogen

* Corresponding author.
E-mail address: sakamoto@prc.tsukuba.ac.jp (M. Sakamoto).

http://dx.doi.org/10.1016/j.nme.2017.05.001

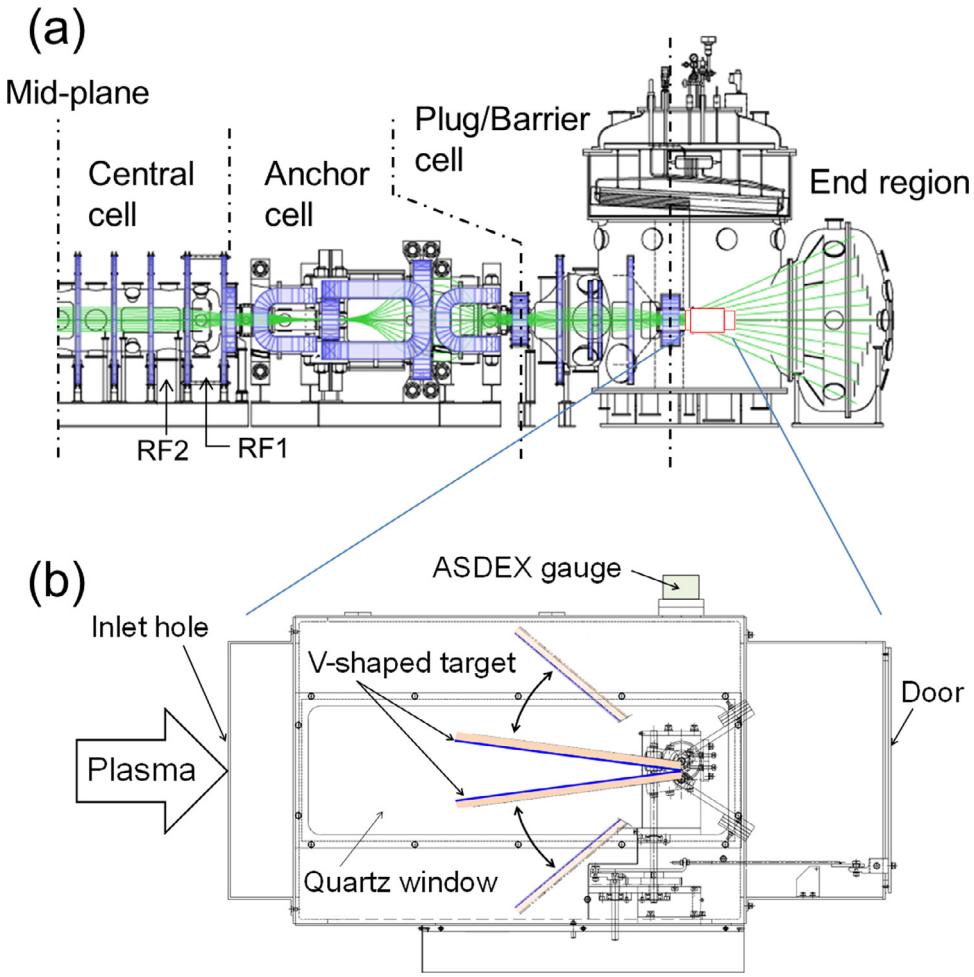

Fig. 1. Schematic views of (a) GAMMA 10/PDX and (b) the D-module.

molecules play an important role in the MAR processes for plasma detachment.

2. Experimental setup

The D-module has been installed in the end region of the GAMMA 10/PDX tandem mirror device [19], which consists of an axisymmetric central-mirror cell (i.e. central cell), anchor cells with minimum-B configuration using baseball coils, plug/barrier cells and end regions as shown in Fig. 1. The end loss plasma is exposed to the D-module. The main plasma is produced in the central cell by using ion cyclotron range of frequency (ICRF) heating, meaning that the ion temperature is rather high (i.e. typically several keV). In the anchor cells next to the central cell, MHD stabilization of the plasma is maintained. In the plug/barrier cells, end loss is prevented by the electrostatic potential which is produced by electron cyclotron heating (ECH) using high power gyrotrons. In this study, however, ECH was not used, since the end loss plasma was used for the divertor simulation. The neutralized gas in the end region is pumped with helium cryopumps.

The D-module consists of a rectangular box (0.5 m square and 0.7 m in length) with an inlet aperture at the front panel and a V-shaped target inside the box as shown in Fig. 1(b). Tungsten target plates with the thickness of 0.2 mm are attached on the V-shaped base. The target size is 0.3 m in width and 0.35 m in length. The open-angle of the V-shaped base can remotely be changed from 15° to 80°. In this study, the open angle was 45°. Additional hydrogen gas can be supplied from the vicinity of the inlet to the target with a different feed rate for each plasma to control the neutral pressure P_n inside the D-module. The neutral pressure is measured with an ASDEX gauge which is installed at an upper part of the D-module. Thirteen Langmuir probes are installed on the upper target plate and two probes are installed between the V-shaped target and the inlet as shown in Fig. 2. The hydrogen Balmer line emissions (H_α and H_β) from the plasma inside the D-module is measured with a spectrometer and a fast camera with an interference filter. The D-module can be moved up and down. In the case of a divertor simulation experiment, it is set on the axis of the plasma.

3. Results and discussion

3.1. Overview of detached hydrogen plasmas

Hydrogen gas is injected into the D-module with a different feed rate shot by shot to obtain dependence of plasma parameters such as electron density (n_e), temperature (T_e) and Balmer line emissions on P_n. The gas feed rate is changed by changing the plenum pressure (i.e. gas pressure in a reservoir tank at the upper stream of a piezoelectric valve). Hydrogen gas was supplied inside the D-module from 300 ms before the plasma production until the end of the plasma. As shown in Fig. 3, P_n becomes constant before the plasma production and then increases due to plasma inflow. The pressure increase must be attributed to suppression of gas flow out of the D-module due to plasma–gas interaction, since contribution of inflow of hydrogen ions on the pressure increase is much smaller.

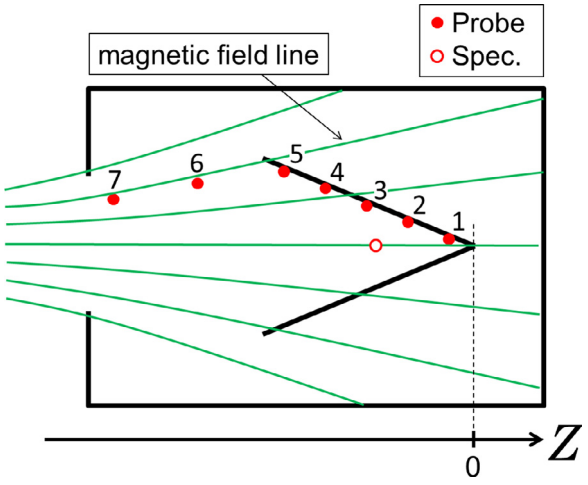

Fig. 2. Arrangement of measurements of Langmuir probes (closed circle) and spectroscopy (open circle). The position of the spectroscopy is 150 mm away from the corner of the V-shaped target. The number above the probe position is a probe number.

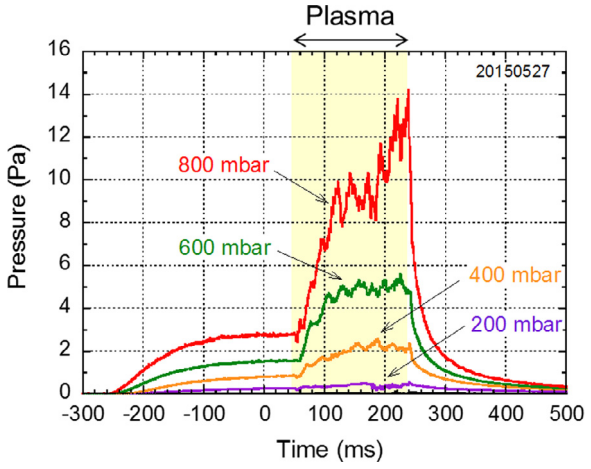

Fig. 3. Time evolution of the neutral pressure inside the D-module, which is measured with an ASDEX gauge, for different plenum pressures of hydrogen gas supply.

Fig. 4(a) shows the line-averaged electron density at the plug cell which is next to the end region. The density increased with increasing P_n until ~4 Pa and then became almost constant. A part of hydrogen gas that flows out of the D-module diffuses to the plug cell, and it is ionized there. As shown in Fig. 4(b), n_e near the inlet of the D-module increased with increasing P_n until ~2 Pa and then became constant, which is a similar tendency to the upstream density at the plug cell. It is noticed that n_e near the inlet of the D-module is about one order of magnitude smaller than that at the plug cell, which is attributed to plasma confinement at the plug cell by a magnetic mirror. The electron density near the corner of the V-shaped target also increased with increasing P_n until ~2 Pa and then decreased, showing a clear density rollover. A rollover of the particle flux to the target (i.e. ion saturation current measured by a Langmuir probe) occurred before the density rollover, which indicates the plasma was detached from the target plate. As shown in Fig. 5, a two-dimensional image of H_β line intensity (I_{H_β}) also indicates the plasma detachment occurred in front of the target. As shown in Fig. 4(c), T_e near the inlet of the D-module decreased from ~30 eV to ~8 eV with increase in P_n and that near the corner of the V-shaped target decreased from ~23 eV to ~2 eV. The ion temperature (T_i) that was measured by a retarding field energy analyzer before setting the D-module on the axis of the plasma

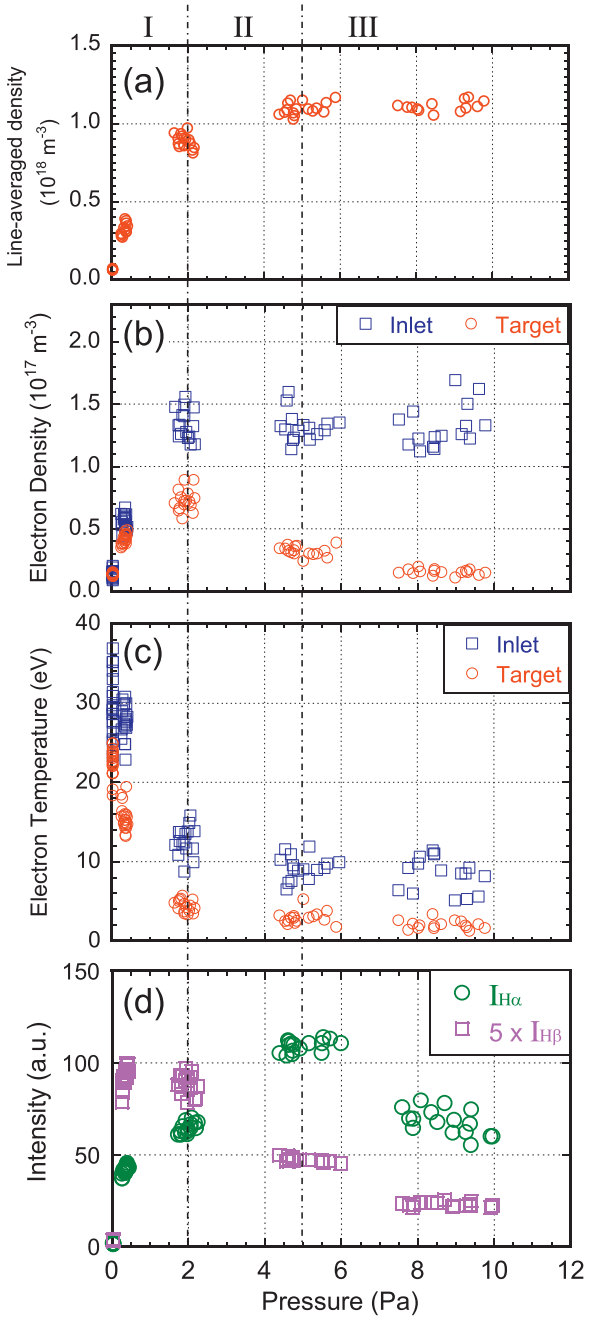

Fig. 4. Neutral pressure dependence of (a) line-averaged electron density at the plug cell, (b) electron density and (c) temperature near the inlet of the D-module (probe No. 7) and the corner of the V-shaped target (Probe No. 1), and (d) Balmer line emissions.

was about 170 eV, which is considered to be almost the same as T_i of the plasma exposed to the D-module without additional gas injection, suggesting that T_i was several times higher than T_e in the case of no gas injection. Fig. 4(d) shows Balmer line intensities as a function of P_n. The trend of I_{H_β} is similar to that of n_e near the corner, but H_α line intensity (I_{H_α}) increased with increasing P_n until ~5 Pa even though the density decreased. The increase in I_{H_α} is considered to be attributed to MAR, which is discussed in the next section.

Fig. 6 shows spatial profiles of T_e and n_e which were measured with Langmuir probes of which arrangement is shown in Fig. 2. The electron temperature decreases as a whole as P_n increases. On the other hand, the behavior of the density profile is rather compli-

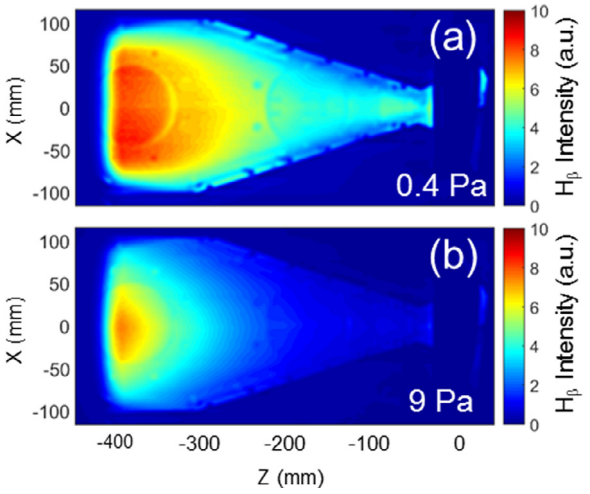

Fig. 5. Images of Balmer β emission in front of the V-shaped target, showing (a) an attached plasma and (b) a detached one. The center wavelength and half maximum full-width of the interference filter attached on the fast camera are 688 nm and 10 nm, respectively. The color scaling of the both images is the same.

Table 1
Processes of molecular activated recombination in hydrogen plasma. The particle H^* refers to electrically excited atomic hydrogen and the notation (v) means a vibrational quantum number.

Label		Reaction
DA-MAR	DA	$H_2(v) + e \rightarrow H^- + H$
	MN	$H^- + H^+ \rightarrow H + H^*$
IC-MAR	IC, CX	$H_2(v) + H^+ \rightarrow H_2^+(v) + H$
	DR	$H_2^+(v) + e \rightarrow H + H^*$
MIC-MAR	IC, CX	$H_2(v) + H^+ \rightarrow H_2^+(v) + H$
	MIC	$H_2(v) + H_2^+(v) \rightarrow H_3^+(v) + H$
	DR	$H_3^+(v) + e \rightarrow 3H, \quad H_2(v) + H^*$

cated due to atomic and molecular processes including ionization and recombination, which depend on not only electron temperature but also electron, neutral atom and molecule densities. The P_n dependence of n_e in front of the target (i.e. $-300 < Z < 0$) is similar to the result of Fig. 4(b) as a whole, suggesting that recombination is dominant in the region in front of the V-shaped target. It is consistent with the result of Fig. 5. The decrease in n_e near the corner of the target (i.e. $-150 < Z < 0$) is remarkable at $P_n \sim 10$ Pa, indicating recombination is enhanced there. This would be a recycling effect at the corner of the target. In the upstream region, it is observed that the position of the density maximum moves upstream as P_n increases, suggesting the ionization front moves upstream as P_n increases.

3.2. Molecular activated recombination in the hydrogen plasma

The atomic and molecular processes that result in MAR have been discussed in many laboratories [1-7, 20-24]. The MAR processes are summarized in Table 1. There are mainly three chains of reactions which lead to MAR. The first chain (refer to as DA-MAR) is the dissociative attachment (DA) of vibrationally excited molecular hydrogen followed by mutual neutralization (MN). The second chain (IC-MAR) is atomic to molecular ion conversion (IC) or charge exchange (CX) followed by the dissociative recombination (DR). In the third chain, the molecular to triatomic molecular ion conversion (MIC-MAR) is followed by two kinds of DR reactions. Fig. 7 shows rate coefficients of DA-MAR ($S_{DA\text{-}MAR}$), IC-MAR($S_{IC\text{-}MAR}$), EIR (S_{EIR}) and ionization (S_{ion}) as a function of T_e, which is calculated by using a CR model [25, 26]. It is noted that reactions of $H_2^+ + e \rightarrow H + H^+ + e$ and $H^- + e \rightarrow H^+ + 2e$, which

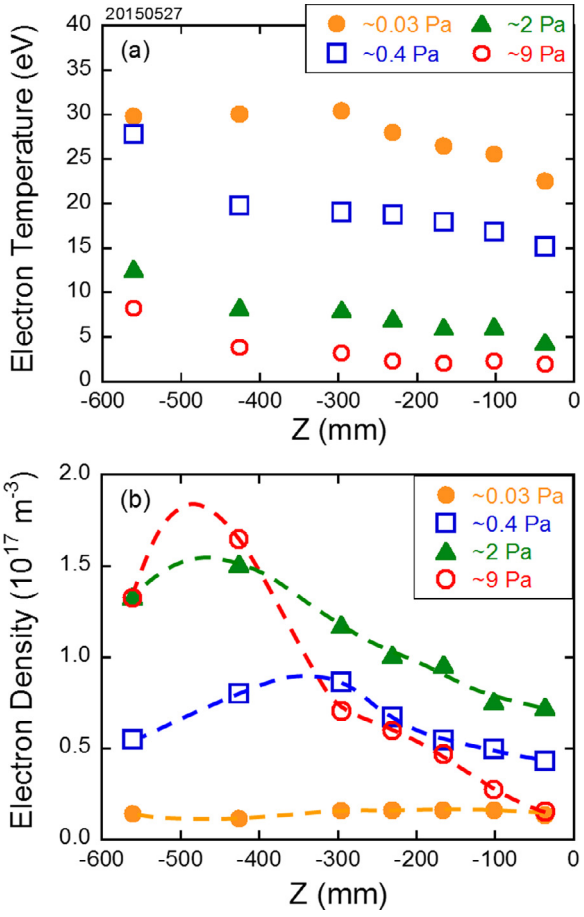

Fig. 6. Profiles of (a) electron temperature and (b) density, which are measured with Langmuir probes for different plenum pressure. The position Z = 0 represents the position of the corner of the V-shaped target.

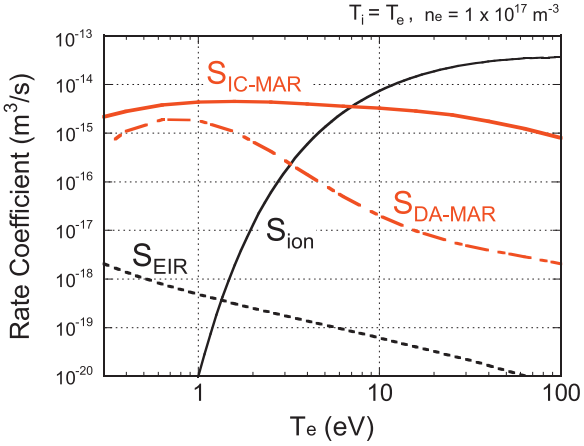

Fig. 7. Rate coefficients of collisional processes as a function of electron temperature: electron-ion recombination (S_{EIR}), ionization (S_{ion}) and molecular activated recombination ($S_{DA\text{-}MAR}$, $S_{IC\text{-}MAR}$), where a vibrational quantum number of hydrogen molecule and the electron density are assumed to be six and 1×10^{17} m^{-3}, and ion temperature is assumed to be the same as electron temperature.

compete with the DA-MAR and IC-MAR processes, are included in the CR model but the MIC-MAR process is not included. It is found that S_{EIR} is low due to low plasma density and it becomes higher than S_{ion} when T_e is less than ~1.3 eV. On the other hand, the MAR rate coefficient becomes much higher than S_{ion} when T_e is less than ~7 eV and hydrogen molecule is vibrationally excited (v

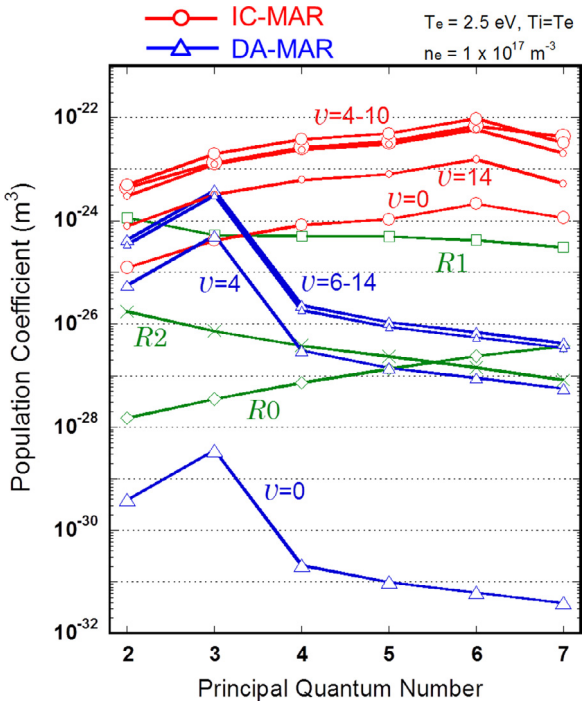

Fig. 8. Comparison of hydrogen population coefficients among processes of R0, R1, R2, IC-MAR and DA-MAR.

$\geq$ 4). It is considered that the density rollover in the experiment was caused by MAR, since the rollover occurred at ~4 eV.

In the MAR processes, excited hydrogen atom is finally produced, which results in enhancement of Balmer line emissions. The population density of them is calculated by using the CR model as follows:

$$n(p) = R_0(p)n_e n_{H^+} + R_1(p)n_e n_H + R_2(p)n_e n_{H_2} + R_{MAR}(p)n_e n_{H_2}, \quad (1)$$

where p is a principal quantum number and n_{H+}, n_H and n_{H_2} are densities of hydrogen ion, neutral hydrogen atom and molecule, respectively. Fig. 8 shows hydrogen population coefficients as a function of p. In this calculation, n_e is 1×10^{17} m^{-3} and T_e is 2.5 eV, which are similar to the experimental parameters with high neutral pressure. Here, T_i is assumed to be the same as T_e. The effect of T_i on the population coefficient is discussed later. Let us consider contribution of each term of the Eq. (1) to $n(3)$ (i.e. I_{H_α}) and $n(4)$ (i.e. I_{H_β}) taking into account n_{H_2} was considerably high in this experiment. When the neutral pressure is 2 Pa, for example, the electron density is around 1×10^{17} m^{-3} as shown in Fig. 4(b), meaning $n_{H_2}/n_{H+} \sim 6 \times 10^3$. As shown in Fig. 8, population coefficients R_0 and R_2 are so small that the first and third terms can be ignored. The second term (i.e. excitation process) may contribute to the population density, but one can consider the MAR process played a dominant role for the population density, since n_{H_2} was high and R_{MAR} is higher than R_1. The population coefficient R_{MAR} of Eq. (1) consists of population coefficients of DA-MAR ($R_{DA\text{-}MAR}$) and IC-MAR ($R_{IC\text{-}MAR}$). In the DA-MAR process, population coefficients with $p = 2$ and 3 are dominant as shown in Fig. 8. In the IC-MAR process, on the other hand, every population coefficient with $p \geq 2$ is high. It is found that sources of I_{H_α} are both processes of DA-MAR and IC-MAR and a source of I_{H_β} is only IC-MAR process. The population coefficient in the DA-MAR process strongly depends on the vibrationally excited state of the hydrogen molecule in the range of the vibrational quantum number $\upsilon = 1$ to

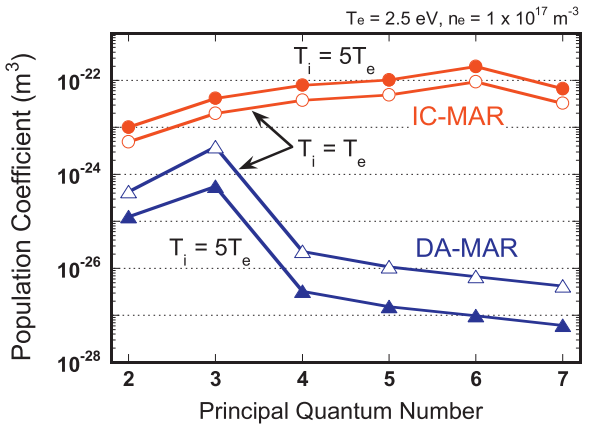

Fig. 9. Comparison of population coefficients for IC-MAR and DA-MAR depending on ion temperature. The vibrational quantum number of hydrogen molecule in this calculation is six.

6 and it is almost the same over $\upsilon = 6$ as shown in Fig. 8. The observation of enhancement of I_{H_α} (Fig. 4(d)) suggests that υ is more than 4–6, since the population coefficient with lower υ is too low to contribute observation of the H_α line emission. The enhancement of I_{H_α} is discussed later.

The ion temperature of the plasma exposed to the D-module is expected to be higher than T_e even in the detachment phase. Fig. 9 shows comparison of $R_{DA\text{-}MAR}$ and $R_{IC\text{-}MAR}$ with $\upsilon = 6$ focusing on the ion temperature. The difference between $R_{DA\text{-}MAR}$ and $R_{IC\text{-}MAR}$ widens as T_i becomes higher than T_e, indicating that IC-MAR becomes the more dominant process than DA-MAR in higher ion temperature range.

Now, we consider atomic and molecular processes in the divertor simulation plasma in front of the V-shaped target dividing into the following three phases: (I) $P_n < 2$, (II) $2 < P_n < 5$, (III) $5 < P_n < 10$. In the phase I, T_e decreases from ~23 eV to ~4 eV and n_e increases from 1.4×10^{16} m^{-3} to 7.3×10^{16} m^{-3} with increase in P_n. Rollover of a particle flux which is evaluated by a Langmuir probe was observed, indicating the plasma detachment started to occur. In the latter of this phase, T_e is so low that IC-MAR becomes more dominant process than ionization as shown in Fig. 7 although n_e still increases. This increase in n_e is considered to be caused by increase in the upstream density shown in Fig. 4(a) and plasma transport from the upstream (i.e. plug cell) to downstream (i.e. inside of the D-module).

In the phase II, n_e and I_{H_β} decreases but I_{H_α} continues to increase with increase in P_n. The increase in I_{H_α} may be caused mainly by the DA-MAR process, since the H_α line emission that is caused by the IC-MAR process is expected to decrease as with decrease in I_{H_β}. This means that the chain reaction in the DA-MAR process was promoted although $S_{DA\text{-}MAR}$ is lower than $S_{IC\text{-}MAR}$ as shown in Fig. 7. The increase in I_{H_α} during decrease in n_e in the phase II suggests that the number of vibrationally excited hydrogen molecules significantly increased, since the reaction products (i.e. excited hydrogen atoms with $p = 3$) increased although the number of reaction partners (i.e. electron and atomic ion) decreased. A key to understand the increase in I_{H_α} during decrease in n_e is MIC-MAR, which produces vibrationally excited molecules to promote the DA reaction in the DA-MAR process. Besides, the MIC-MAR process impedes IC-MAR by consuming molecule ions that are used for IC-MAR. Although a rate coefficient of MIC-MAR is not available and quantitative discussion cannot be done, one can consider that if the MIC-MAR process does not work IC-MAR is the dominant process as shown in Fig. 8 and I_{H_α} and I_{H_β} would show similar trend in the neutral pressure dependence. The op-

posite trend in I_{H_α} and I_{H_β} behaviors in the phase II suggests that the chain reaction in the DA-MAR process is promoted by increase in the vibrationally excited molecules that are produced by MIC-MAR. The H_α intensity decreases in the phase III, which may be caused by decrease in n_e due to enhancement of the plasma detachment.

4. Conclusion

The hydrogen gas injection to the divertor simulation plasma in the D-module has been done to investigate the plasma detachment process. The electron temperature in front of the V-shaped target in the D-module decreased with increase in the neutral pressure and the density rollover occurred in front of the target as a whole around 2 Pa, indicating the plasma was detached from the target plate, which was caused by MAR. In the region near the corner of the target, in particular, the electron temperature decreased to ~2 eV and decrease in the density was remarkable due to enhancement of the recycling at the corner of the target. After the density rollover, I_{H_β} decreased as with the density but I_{H_α} continued to increase with the neutral pressure, indicating that DA-MAR is the more dominant process than IC-MAR although the rate coefficient of DA-MAR is lower than that of IC-MAR. It is considered that increase in I_{H_α} and decrease in I_{H_β} are caused by promotion of the MIC-MAR process, meaning the IC-MAR process is impeded by promotion of the MIC-MAR process and the DA reaction in the DA-MAR process is promoted by increase in the number of vibrationally excited molecules produced by MIC-MAR.

Acknowledgment

The authors would like to thank the members of the GAMMA 10 group in University of Tsukuba for their support in the experiments. This work is performed with the support of NIFS Collaborative Research Program (NIFS13KUGM083 and NIFS16KUGM119).

References

[1] R.K. Janev, J. Nucl. Mater. 121 (1884) 10–16.
[2] D.E. Post, J. Nucl. Mater 220-222 (1995) 143–157.
[3] S.I. Krasheninnikov, A.Yu. Pigarov, D.J. Sigmar, Phys. Lett. A 214 (1996) 285–291.
[4] A.Yu. Pigarov, S.I. Krasheninnikov, Phys. Lett. A 222 (1996) 251–257.
[5] S.I. Krasheninnikov, Phys. Scr. T96 (2002) 7–15.
[6] A.Yu. Pigarov, Phys. Scr. T96 (2002) 16–31.
[7] R.K. Janev, Phys. Scr. T96 (2002) 94–101.
[8] N. Ohno, et al., Phys. Rev. Lett. 81 (1998) 818–821.
[9] N. Ezumi, et al., J. Nucl. Mater. 266-269 (1999) 337–342.
[10] A. Tonegawa, et al., J. Nucl. Mater. 313-316 (2003) 1046–1051.
[11] S. Kado, et al., J. Nucl. Mater. 337-339 (2005) 166–170.
[12] A. Tonegawa, et al., Jpn. J. Appl. Phys. 45 (2006) 8212–8216.
[13] A. Okamoto, et al., J. Nucl. Mater. 363-365 (2007) 395–399.
[14] J. Terry, et al., Phys. Plasmas 5 (1997) 1759–1766.
[15] U. Franz, et al., J. Nucl. Mater. 290-293 (2001) 367–373.
[16] Y. Nakashima, et al., Trans. Fusion Sci. Technol. 63 (2013) 100.
[17] M. Sakamoto, et al., Trans. Fusion Sci. Technol. 63 (2013) 188.
[18] Y. Nakashima, et al., J. Nucl. Mater. 463 (2015) 537.
[19] M. Inutake, et al., Phys. Rev. Lett. 55 (1985) 939.
[20] J.M. Wadehra, J.N. Bardsley, Phys. Rev. Lett. 41 (1978) 1795–1798.
[21] K.C. Kulander, M.F. Guest, J. Phys. B: Atom. Molec. Phys. 12 (1979) L501–L504.
[22] J.B.A. Mitchell, et al., Phys. Rev. Lett. 51 (1983) 885–888.
[23] E.M. Hollmann, A.Yu. Pigarov, Phys. Plasmas 9 (2002) 4330–4339.
[24] H. Yazawa, et al., Jpn. J. Appl. Phys. 45 (2006) 8208–8211.
[25] T. Fujimoto, K. Sawada, K. Takahata, J. Appl. Phys. 66 (1989) 2315–2319.
[26] K. Sawada, T. Fujimoto, Contrib. Plasma Phys 42 (2002) 603–607.